

Neutralino Dark Matter in MSSM Models with Non-Universal Higgs Masses

Pearl Sandick

*Theory Group and Texas Cosmology Center,
The University of Texas at Austin, TX 78712, USA*

Abstract.

We consider the Minimal Supersymmetric Standard Model (MSSM) with varying amounts of non-universality in the soft supersymmetry-breaking contributions to the Higgs scalar masses. In addition to the constrained MSSM (CMSSM) in which these are universal with the soft supersymmetry-breaking contributions to the squark and slepton masses at the input GUT scale, we consider scenarios in which both the Higgs masses are non-universal by the same amount (NUHM1), and scenarios in which they are independently non-universal (NUHM2). As the lightest neutralino is a dark matter candidate, we demand that the relic density of neutralinos not be in conflict with measurements by WMAP and others, and examine the viable regions of parameter space. Prospects for direct detection of neutralino dark matter via elastic scattering in these scenarios are discussed.

Keywords: Supersymmetry, Dark Matter

PACS: 11.30.Pb, 95.35.+d

INTRODUCTION

TeV-scale Supersymmetry (SUSY) is one of the most compelling theories of physics beyond the Standard Model for several reasons: it facilitates unification of the gauge couplings, as expected in Grand Unified Theories (GUTs); it stabilizes the Higgs vacuum expectation value, offering a solution to the related hierarchy and naturalness problems of the Standard Model; and it predicts a light Higgs boson, as expected from electroweak precision measurements. In addition, if R-parity is conserved, the lightest supersymmetric particle (LSP) is stable, and, if uncharged, is therefore a natural particle candidate for astrophysical cold dark matter.

Phenomenologically, one of the most-studied versions of the Minimal Supersymmetric Standard Model (MSSM) is the constrained MSSM (CMSSM), in which the soft supersymmetry-breaking contributions to the masses of the SUSY partners of the quarks and leptons and the Higgs scalars are universal at some GUT input scale, as motivated by minimal supergravity. However, while the CMSSM may be the simplest scenario, it is by no means the most plausible version of the MSSM. Here, we present the results of recent studies of models with non-universal supersymmetry-breaking contributions to the Higgs masses [1, 2].

The CMSSM is parametrized by four continuous parameters specified at the SUSY GUT scale and a sign choice: the universal gaugino mass, $m_{1/2}$, the universal scalar mass, m_0 , the universal value for the trilinear couplings, A_0 , the ratio of the Higgs vacuum expectation values, $\tan(\beta)$, and the sign of the Higgs mixing parameter, μ . In this scenario, the GUT-scale values of the effective Higgs masses are $m_1 = m_2 = m_0$, and the electroweak vacuum conditions fix $|\mu|$ and the pseudoscalar Higgs mass, m_A . In the NUHM1, the effective Higgs masses are assumed to be universal at the GUT scale, though the universality with m_0 is relaxed. One more input parameter, in addition to those of the CMSSM, is required, and may be taken as μ , m_A , or the GUT-scale value of the Higgs masses $m_1 = m_2$. Similarly, in NUHM2 models, no relation between m_1 , m_2 , and m_0 is assumed. This scenario may be parametrized by additional inputs μ and m_A , or by both GUT-scale effective Higgs masses.

In each scenario, the renormalization group equations of the MSSM are used to determine the low-scale observables, and constraints from colliders and cosmology are applied. We assume that the lightest neutralino is the dark matter candidate, calculate its abundance, and determine the prospects for direct detection for models which are phenomenologically and cosmologically viable, i.e. models not excluded by constraints from colliders, and where the upper limit on the relic density of neutralinos is respected. Direct detection experiments derive limits on the dark matter-nucleon scattering cross section under the assumption that the local density of cold dark matter comes from a single source, that is, one particle species is responsible for the entire dark matter abundance, Ω_{CDM} . However, this may not be the

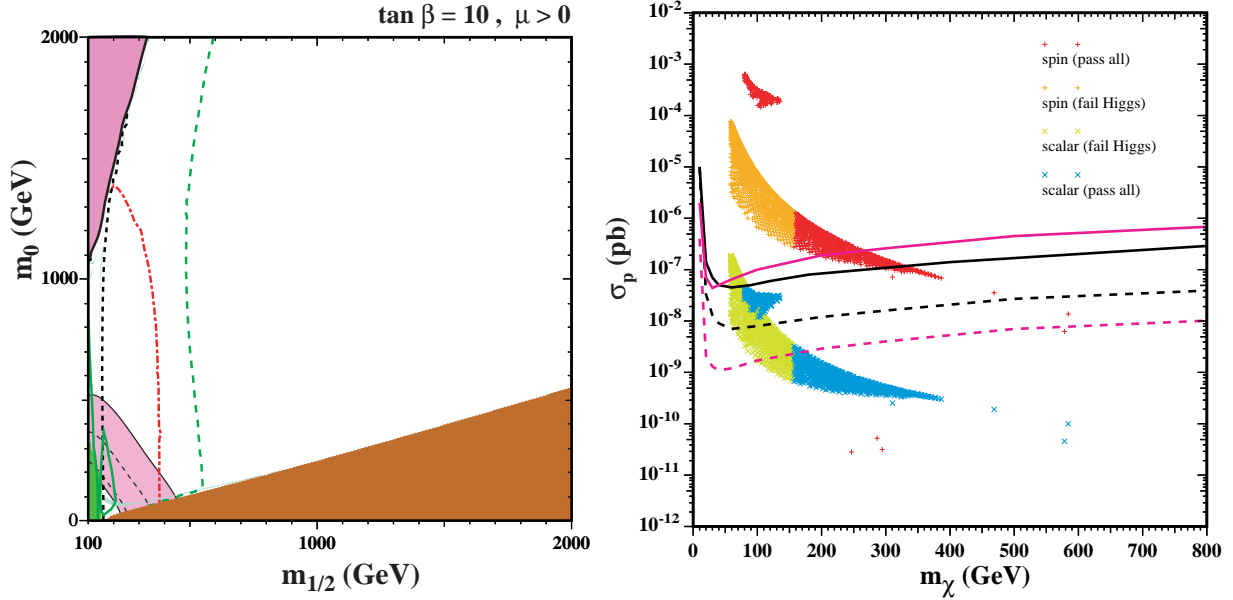


FIGURE 1. In the left panel, we show the CMSSM $(m_{1/2}, m_0)$ plane for $\tan\beta = 10$, $A_0 = 0$, and $\mu > 0$ with the corresponding neutralino-nucleon elastic scattering cross sections as functions of neutralino mass in the right panel. Constraints are as discussed in the text. For further details on this and other figures, please refer to [2].

case. If the calculated neutralino abundance is less than the WMAP central value [3], Ω_{CDM} , we assume a secondary source of cold dark matter, and rescale the neutralino-nucleon cross sections by a factor Ω_χ/Ω_{CDM} in order to compare our calculated elastic scattering cross sections with limits from direct searches.

THE CMSSM

In Fig. 1, we present the neutralino-nucleon elastic scattering cross section as a function of neutralino mass for one slice of the CMSSM parameter space. In the left panel, we show the $(m_{1/2}, m_0)$ plane for $\tan\beta = 10$, $A_0 = 0$, and $\mu > 0$, with the corresponding neutralino-nucleon elastic scattering cross sections for phenomenologically-viable regions in the panel on the right. The region excluded because the LSP is a charged $\tilde{\tau}$ is shaded brown, and, at large m_0 , that where electroweak symmetry breaking cannot be obtained (resulting in unphysical $\mu^2 < 0$), in pink. The red dot-dashed contour corresponds to a Higgs mass of 114 GeV. At lower $m_{1/2}$ the Higgs boson would be lighter, which is excluded by its non-observation at LEP [4]. We also plot a black dashed contour for $m_{\chi^\pm} = 104$ GeV, with the region at lower $m_{1/2}$ also excluded by LEP. The green shaded region at very low $m_{1/2}$ and m_0 is disfavored by the measured branching ratio for $b \rightarrow s\gamma$ [5], while the light pink shaded region is favored by the measurement of the muon anomalous magnetic moment at the $2\text{-}\sigma$ level [6]. Finally, in the turquoise shaded regions, the relic density of neutralinos falls within the WMAP range [3]. For the value $\tan\beta = 10$ presented here, the only cosmologically-preferred regions are the coannihilation strip, bordering the $\tilde{\tau}$ -LSP region, and the focus-point region at large m_0 , where μ is small and the LSP is a mixed bino-Higgsino state. Over the bulk of the plane, the relic density of neutralinos exceeds the value measured by WMAP by more than $2\text{-}\sigma$. There are, however, slim strips where $\Omega_\chi h^2$ is below the WMAP range, which lie between the WMAP-preferred strips and the excluded regions they border.

Turning to the right panel of Fig. 1, we have separated out the cross section for spin-dependent (SD) scattering (red/orange) and the scalar or spin-independent (SI) cross section (blue/green). Here and throughout, we assume the current limits on the branching ratios of $B \rightarrow \mu\mu$ and $b \rightarrow s\gamma$ are respected, as well as the lower limit on the chargino mass, and differentiate regions in which the scalar Higgs mass is below the LEP limit (green/orange) and above the LEP limit (blue/red). Here, the Higgs mass is below the LEP limit in the coannihilation strip at low $m_{1/2}$, corresponding to low m_χ . Both the SI and SD cross sections in the upper right panel contain two distinct regions, that arising from the focus-point region at $m_\chi \lesssim 150$ GeV and relatively large σ , and a more extended region due to the coannihilation strip.

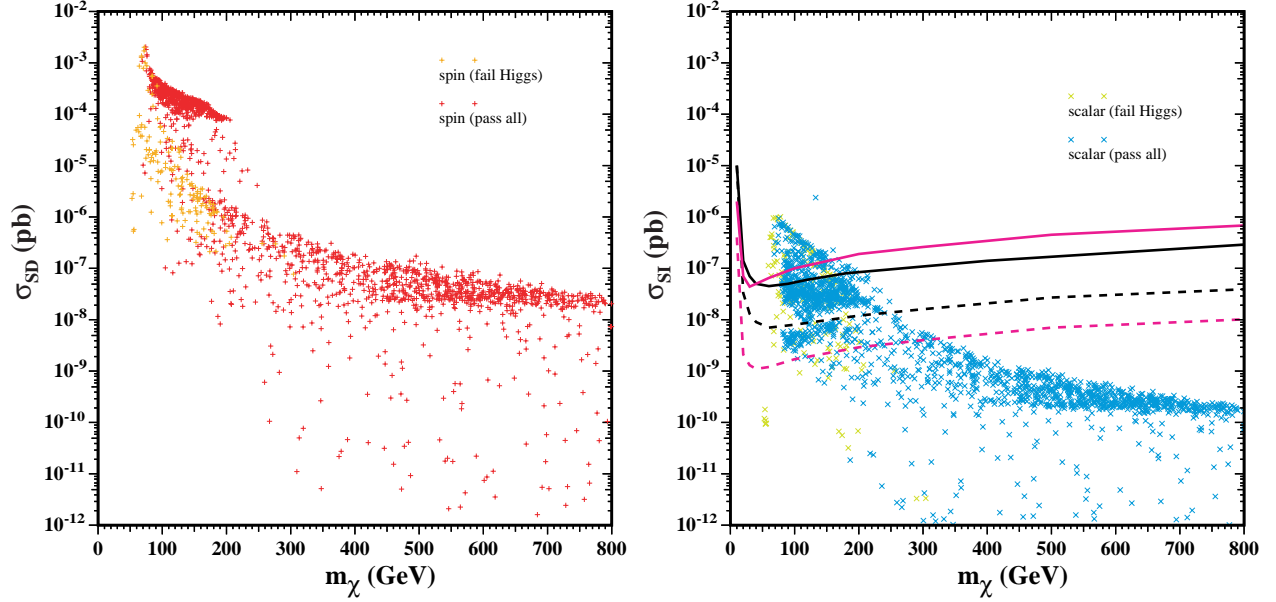


FIGURE 2. Here we present the entire potential range of neutralino-nucleon elastic scattering cross sections as functions of neutralino mass for the CMSSM, with $5 \leq \tan\beta \leq 55$, $100 \text{ GeV} \leq m_{1/2} \leq 2000 \text{ GeV}$, $0 \leq m_0 \leq 2000 \text{ GeV}$, and $-3m_{1/2} \leq A_0 \leq 3m_{1/2}$. We consider $\mu < 0$ only for $\tan\beta < 30$. On the left are the cross sections for SD scattering, and on the right are those for SI scattering. Also shown in the right panel are upper limits on the SI dark matter scattering cross section as specified in the text.

In the coannihilation strip, $50 \text{ GeV} < m_\chi < 400 \text{ GeV}$, where the lower limit on m_χ is a result of the LEP constraint on the chargino mass, and the upper limit on m_χ corresponds to the end-point of the coannihilation strip for $\tan\beta = 10$. At larger values of $\tan\beta$, we also find a rapid annihilation funnel in the CMSSM parameter space.

We also plot in the right panel of Fig. 1 the limits on the SI cross section from CDMS II [7] (solid black line) and XENON10 [8] (solid pink line), as well as the sensitivities projected for XENON100 [9] (or a similar 100-kg liquid noble-gas detector such as LUX, dashed pink line) and SuperCDMS at the Soudan Mine [10] (dashed black line). One can see that the SD cross sections are generally larger than SI cross sections, though current upper limits are larger than 10^{-2} pb .

At very low $m_{1/2}$, CDMS II and XENON10 have definitively excluded some of the region where m_h is below the LEP limit. We show this explicitly in the left panel by plotting the reach of current and future direct detection experiments in the parameter space. Here and in subsequent parameter space scans, we display contours of scalar neutralino-nucleon scattering cross section, scaled by $\Omega_\chi/\Omega_{\text{CDM}}$ if necessary, of $5 \times 10^{-8} \text{ pb}$ (solid green contours) and 10^{-9} pb (dashed green contours). A cross section of $5 \times 10^{-8} \text{ pb}$ is currently excluded by XENON10 for $m_\chi = 30 \text{ GeV}$ and by CDMS II for $m_\chi = 60 \text{ GeV}$, and will be probed by SuperCDMS for m_χ up to $\sim 1000 \text{ GeV}$. Tonne-scale liquid noble-gas detectors such as the proposed XENON1T or a similar detector mass for LUX/ZEP will be sensitive to scalar cross sections below 10^{-9} pb for all neutralino masses in the range $10 \text{ GeV} \lesssim m_\chi \lesssim \text{a few TeV}$ [9]. These detectors will be sensitive to cross sections below 10^{-10} pb over much of the preferred mass range $m_\chi \sim \mathcal{O}(100) \text{ GeV}$.

Of course, we would like to know the range of potential neutralino-nucleon elastic scattering cross sections that are possible in the CMSSM. In Fig. 2, we scan over all CMSSM parameters, with SD neutralino-nucleon elastic scattering cross sections in the left panel, and SI cross sections in the right panel. One can see that, in both the SI and SD cases, there is an upper limit on the cross section as a function of neutralino mass. Focusing on the SI elastic scattering cross sections, at low $m_\chi < 300 \text{ GeV}$, cross sections generally exceed 10^{-9} pb . The largest cross sections, already excluded by CDMS and XENON10, come primarily from the focus point region at large $\tan\beta$.

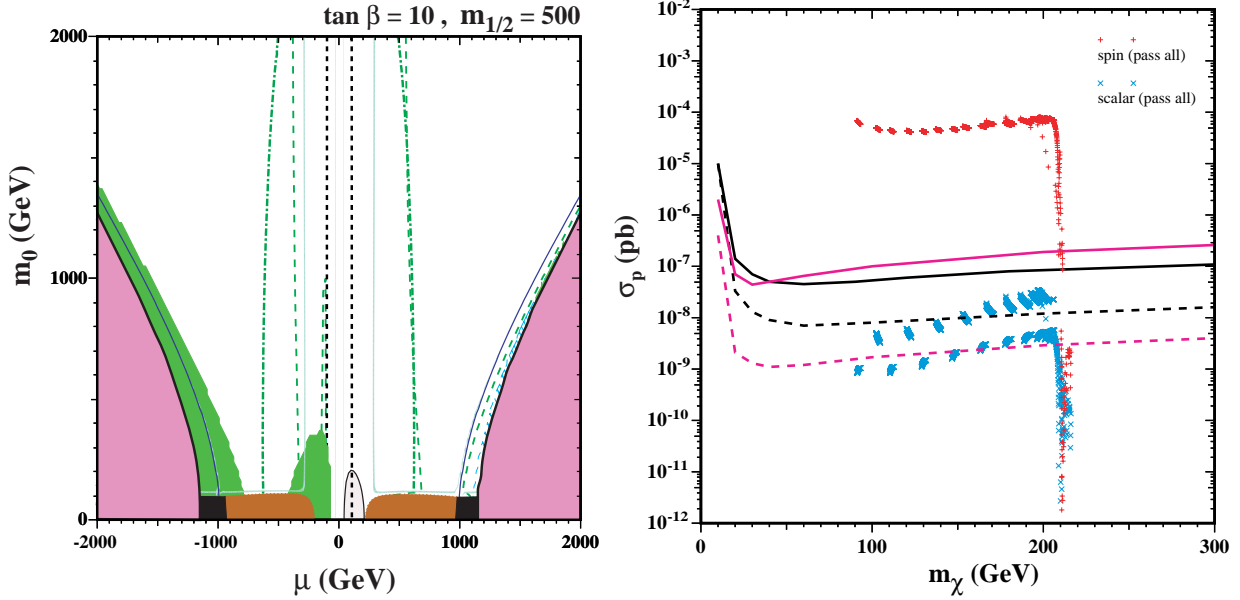


FIGURE 3. The left panel shows an NUHM1 (μ, m_0) plane for $m_{1/2} = 500$ GeV, $\tan\beta = 10$, and $A_0 = 0$. The right panel shows the corresponding neutralino-nucleon elastic scattering cross sections for phenomenologically-viable models.

NUHM1 MODELS

In the NUHM1, the parameter space is expanded by one dimension, resulting in additional regions where all constraints are satisfied: *selectron* coannihilation strips and *crossover* regions. In the left panel of Fig. 3, we show an example slice of NUHM1 parameter space, a (μ, m_0) plane. The cosmologically-preferred (turquoise) shaded strips, from large to small $|\mu|$, are: rapid annihilation funnels, where $m_\chi \approx m_A/2$, rising up at $|\mu| \approx 1000$ GeV and arcing outwards (note that for $\mu < 0$ the entire funnel is excluded by the branching ratio of $b \rightarrow s\gamma$); selectron coannihilation strips bordering the black excluded selectron-LSP regions at low m_0 ; stau coannihilation strips between $|\mu| \approx 1000$ GeV and $|\mu| \approx 300$ GeV at low m_0 ; and vertical crossover strips at $|\mu| \approx 300$ GeV, where the LSP is in a mixed bino-Higgsino state. The resulting neutralino-nucleon cross sections are shown in the right panel of Fig. 3. Most cross sections are clustered at $m_\chi \sim 215$ GeV due to the fact that the lightest neutralino is bino-like over most of the plane. The smallest cross sections shown come from the funnel or other regions where the relic density is suppressed (and therefore the cross section is scaled). The largest cross sections come from the crossover strip, near its intersection with the coannihilation strip, and for $\mu > 0$. Between the crossover strips, moving to smaller $|\mu|$, m_χ decreases, as does the relic density of neutralinos, leading to strips in the right panel of scaled cross sections, with m_χ decreasing to ≈ 100 GeV.

In Fig. 4, we show a different slice of parameter space, this time the $(m_A, m_{1/2})$ plane, for $m_0 = 500$ GeV, $\tan\beta = 10$, $\mu > 0$, and $A_0 = 0$. The triangular allowed region is bounded by the constraint on the branching ratio of $b \rightarrow s\gamma$ at small m_A , the appearance of a slepton LSP at large $m_{1/2}$, and the absence of a consistent electroweak vacuum at larger m_A and smaller $m_{1/2}$. The diagonal blue line indicates where $m_\chi = m_A/2$. On each side of this contour there is a narrow rapid-annihilation funnel strip where the relic density falls within the WMAP range. The funnel extends only to $m_{1/2} \approx 1200$ GeV, and therefore $m_\chi \lesssim 550$ GeV for this region. There is another WMAP strip in the focus-point region close to the electroweak vacuum boundary, where the LSP is more Higgsino-like. The displayed part of the focus-point strip is cut off at $m_A = 2000$ GeV, corresponding to $m_\chi \lesssim 600$ GeV; larger values of m_χ would be allowed if one considered larger values of m_A . Apart from the region between this strip and the boundary, and between the funnel strips, the relic LSP density would exceed the WMAP range. The limit on the branching ratio of $b \rightarrow s\gamma$ is important at very low m_A and m_0 , but it is the constraint on the Higgs mass (red dot-dashed curve, roughly horizontal at $m_{1/2} = 400$ GeV) that places a lower limit on the expected LSP mass for the funnel region of $m_\chi \sim 160$ GeV.

The green dashed contour in the left panel of Fig. 4, indicating a future sensitivity to spin-independent dark matter scattering at the level of 10^{-9} picobarns, runs mainly through the region where the relic density exceeds the WMAP upper limit. SuperCDMS at Soudan would be sensitive to much of the focus-point region shown in the panel on the

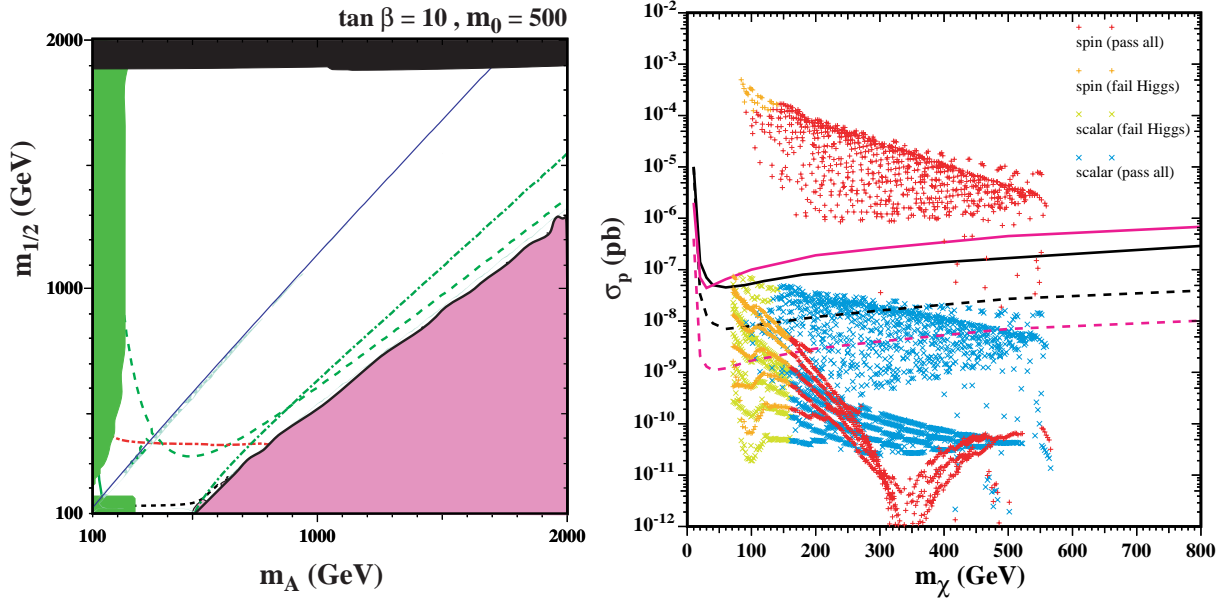


FIGURE 4. The left panel shows an NUHM1 $(m_A, m_{1/2})$ plane for $m_0 = 500$ GeV, $\tan\beta = 10$, and $A_0 = 0$. The right panel shows the corresponding neutralino-nucleon elastic scattering cross sections for phenomenologically-viable models.

left, but a more advanced detector would be required if the relic density of neutralinos is below the WMAP range. Unfortunately, even if neutralinos make up all the dark matter in the universe, much of the funnel region will remain out of reach, even to next-generation direct detection experiments. Points associated with the funnel with cross sections larger than 10^{-9} pb fail the Higgs mass constraint.

The right panel of Fig. 4 displays the scattering cross sections for phenomenologically-viable points in the left plane. The fact that scalar cross sections in the funnel region are generally smaller than those in the focus-point region is reflected in the lower cutoff on the LSP mass, $m_\chi \lesssim 550$ GeV, seen in the right panel for the points with $\sigma_{SI} \lesssim \text{few} \times 10^{-10}$ pb. In the focus-point region, the LSP is in a mixed state with $m_\chi \lesssim 600$ GeV, and the cross section may be much larger: by two orders of magnitude for the SI cross section, and four orders of magnitude for the SD cross section. These large cross sections at large m_χ have no counterparts in the CMSSM, where mixed states in the focus-point region are much lighter. Furthermore, in the CMSSM, the focus point is reached only at large m_0 , whereas here it appears even at fixed $m_0 = 500$ GeV. CDMS II and XENON10 are already beginning to probe the large scalar cross sections in the focus-point region, with a few points at very low $m_{1/2}$ already being excluded, as one can see directly in the right panel¹. We also note that there are points in the right panel with very low cross sections even though they have $m_\chi < 150$ GeV, which also have no counterparts in the CMSSM. These points are associated with the funnel and their cross sections are scaled down due to the low relic density in that region.

A new feature seen in this plot is the near-vanishing of the spin-dependent cross section when $m_\chi = 350$ GeV. This feature is associated with the funnel region where elastic scattering cross sections are substantially lower than those of the focus-point region. However, near $m_\chi = 350$ GeV there is the possibility for a complete cancellation in the SD neutralino-nucleon elastic scattering matrix elements when the spin contribution from up quarks cancels that due to down and strange quarks. The exact position of the cancellation is sensitive to the values of the spin matrix elements adopted, but the existence of the cancellation is robust. Of course, as we present here the cross sections for scattering on protons, the cross sections for scattering on neutrons will not exhibit a cancellation in the same place.

¹ We note these points also have $m_h < 114$ GeV and are within the solid green contour in the left panel of Fig. 4 at very low values of $m_{1/2}$ and m_A .

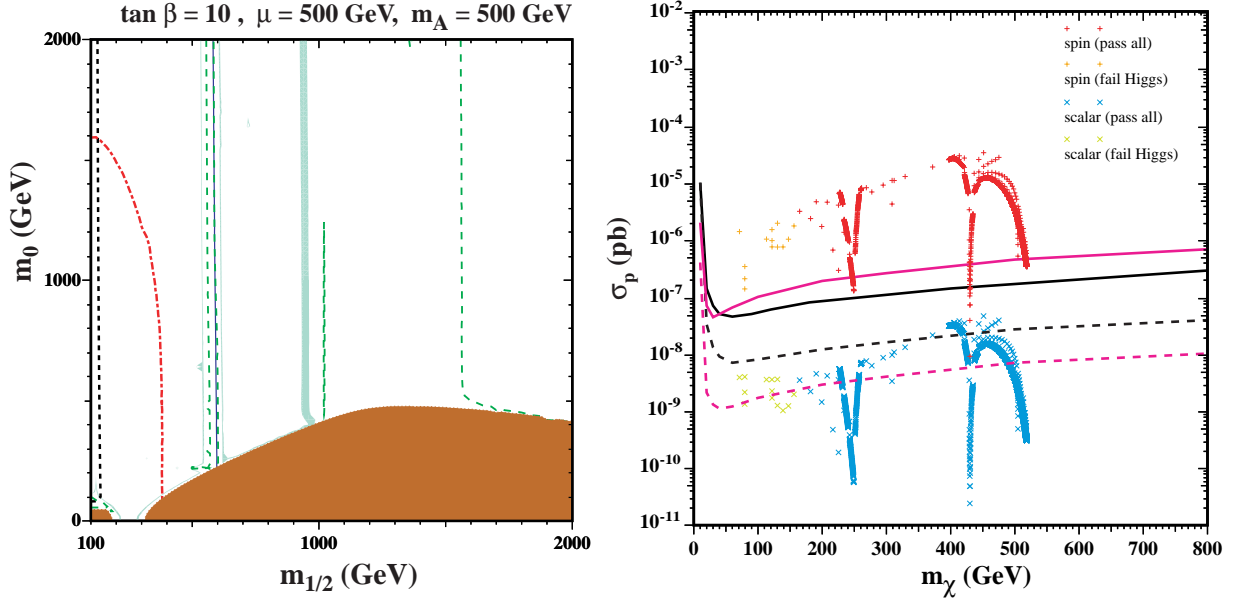


FIGURE 5. The left panel shows an NUHM2 $(m_{1/2}, m_0)$ plane for $\mu = m_A = 500$ GeV, $\tan\beta = 10$, and $A_0 = 0$. The right panel shows the corresponding neutralino-nucleon elastic scattering cross sections for phenomenologically-viable models.

NUHM2 MODELS

As already discussed, the NUHM2 has two parameters in addition to those already present in the CMSSM, which may be taken as free choices of both the quantities m_A and μ . As the number of parameters is relatively large, a systematic survey of the NUHM2 parameter space is quite complex. Here we exhibit one plane of parameter space whose features we compare with the CMSSM and NUHM1. For further discussions of direct detection cross sections in the NUHM2, see [2, 11].

We display in the left panel of Fig. 5 a sample NUHM2 $(m_{1/2}, m_0)$ plane with $\tan\beta = 10$ and fixed $m_A = 500$ GeV and $\mu = 500$ GeV, which reveals a few interesting new features. As in the CMSSM, there is a region in the plane at large $m_{1/2}$ and small m_0 which is forbidden because the lighter stau is the LSP. Just above this forbidden region, as in the CMSSM, there is a stau-coannihilation strip. However, jutting up from this strip at $m_{1/2} \sim 600$ GeV and ~ 950 GeV, there are vertical strips where the relic density of neutralinos falls within the WMAP range. The double strips at $m_{1/2} \sim 600$ GeV form a rapid-annihilation funnel on either side of the (solid blue) contour where $m_A = 2m_\chi$. Again, such funnels appear only at large $\tan\beta$ in the CMSSM, but the freedom to choose different values of m_A in the NUHM2 permits the appearance of a rapid-annihilation funnel also at the low value $\tan\beta = 10$ shown here. The other vertical WMAP strip appears because, as $m_{1/2}$ increases relative to μ (which is fixed here), the Higgsino fraction of the lightest neutralino increases, which in turn increases the annihilation rate, decreasing the relic density. In this case, this results in a crossover region when $m_{1/2} \sim 950$ GeV. At slightly larger $m_{1/2} = 1020$ GeV, the lightest and next-to-lightest neutralinos are nearly degenerate in mass, and rapid coannihilations (through Z-exchange) result in a narrow region with suppressed relic density, and therefore a suppressed scalar cross section.

These novel regions are clearly visible in the right panel of Fig. 5. The elastic scattering cross sections do not vary rapidly as m_χ increases, until the funnel region at $m_\chi \sim 250$ GeV is reached. The "V"-shaped suppression in the cross section arises from the increasing value of m_0 as one rises up the funnel. The two sides of the funnel approach each other as m_0 increases, eventually joining together and resulting in a minimum value where the two sides of the funnel meet (at a value of $m_0 > 2000$ GeV). After this excitement, the cross section continues to rise gradually as one follows the coannihilation strip, until the crossover strip is reached at $m_\chi \sim 400$ GeV. Here the cross section decreases again as m_0 increases, to values even smaller than in the rapid-annihilation funnel, before rising again and finally declining towards the end of the coannihilation strip. Note that the entire region to the right of the transition strip is viable, albeit with a relic density below the WMAP range. The cross section is therefore reduced due to scaling. Because the neutralino is predominantly Higgsino-like here, its mass is given by μ rather than $m_{1/2}$, and so we see in the right

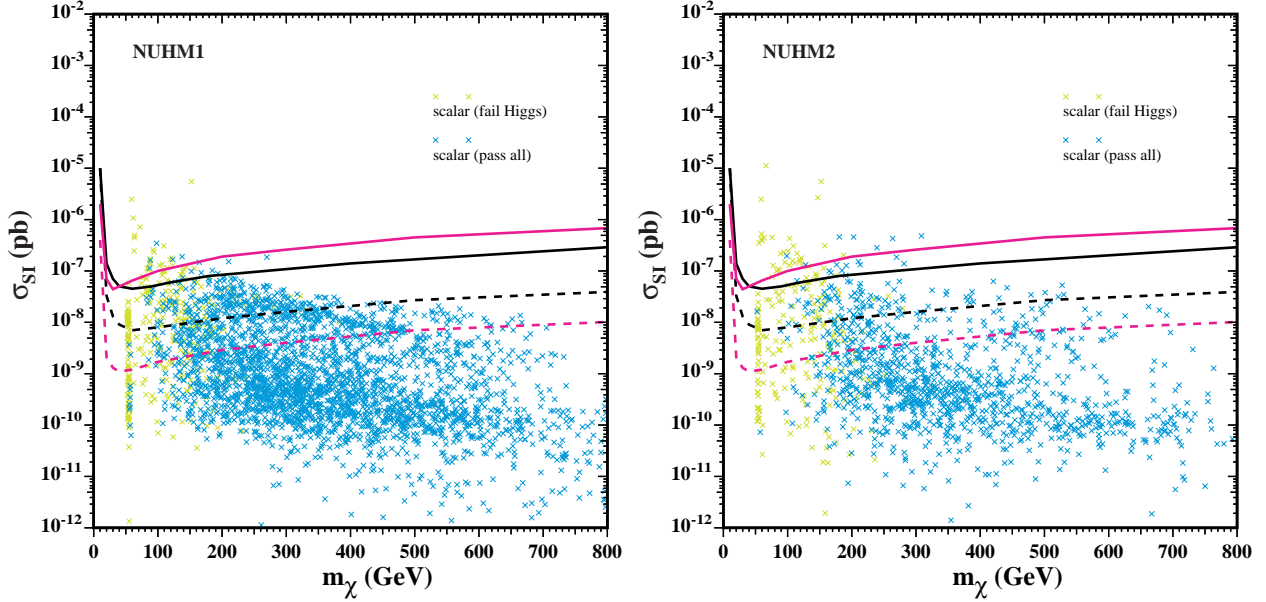


FIGURE 6. We show the entire potential ranges in the NUHM1 and NUHM2 of the SI neutralino-nucleon cross sections with respect to neutralino mass. In both plots, we scan $5 \leq \tan\beta \leq 55$, $100 \text{ GeV} \leq m_{1/2} \leq 2000 \text{ GeV}$, $0 \leq m_0 \leq 2000 \text{ GeV}$, and $-3m_{1/2} \leq A_0 \leq 3m_{1/2}$. The GUT-scale values of m_1 and m_2 are in the range $(-2000, 2000) \text{ GeV}$, with $m_1 = m_2$ in the NUHM1.

panel that the largest values of m_χ correspond to our choice of fixed μ .

SUMMARY

Finally, in Fig. 6 we show the entire potential ranges for the SI neutralino-nucleon elastic scattering cross section as a function of neutralino mass in the NUHM1 (left) and NUHM2 (right). Because of the additional freedom in the Higgs sector, and since the SI elastic scattering cross sections receive important contributions from Higgs exchange, there is more variability in the cross sections in the NUHM1 and NUHM2 than in the CMSSM. This is clear from comparison with the corresponding CMSSM panel in Fig. 2. Differences are due primarily to the appearance of additional regions of parameter space in NUHM models where the lightest neutralino is in a mixed bino-Higgsino state, such as the crossover region.

In both the NUHM1 and NUHM2, we find significantly larger cross sections at larger m_χ than would be expected in the CMSSM. These cross sections may be probed by the next generation of direct detection experiments for m_χ as large as $\sim 700 \text{ GeV}$, while in the CMSSM there is no hope for detection with these instruments for $m_\chi \gtrsim 350 \text{ GeV}$. In addition, we find viable points at very low m_χ with rather low cross sections. If nature has given us a neutralino of this character, then we may not directly detect dark matter for some time, but the LHC may find supersymmetric particles fairly quickly. In either scenario, we will know that the CMSSM is not an adequate description of nature. We look forward to results from both collider experiments and the next generation of dark matter direct detection experiments, which may give us some interesting hints about the mechanism of supersymmetry breaking.

ACKNOWLEDGMENTS

This material is based upon work supported by the National Science Foundation under Grant No. PHY-0455649.

REFERENCES

1. J. R. Ellis, K. A. Olive and P. Sandick, Phys. Rev. D **78**, 075012 (2008) [arXiv:0805.2343 [hep-ph]].
2. J. Ellis, K. A. Olive and P. Sandick, arXiv:0905.0107 [hep-ph].
3. J. Dunkley *et al.* [WMAP Collaboration], Astrophys. J. Suppl. **180**, 306 (2009) [arXiv:0803.0586 [astro-ph]]; E. Komatsu *et al.* [WMAP Collaboration], Astrophys. J. Suppl. **180**, 330 (2009).
4. Joint LEP 2 Supersymmetry Working Group, *Combined LEP Chargino Results, up to 208 GeV*, http://lepsusy.web.cern.ch/lepsusy/www/inos_moriond01/charginos_pub.html; LEP Higgs Working Group for Higgs boson searches, OPAL Collaboration, ALEPH Collaboration, DELPHI Collaboration and L3 Collaboration, Phys. Lett. B **565** (2003) 61 [arXiv:hep-ex/0306033]. *Search for neutral Higgs bosons at LEP*, paper submitted to ICHEP04, Beijing, LHWG-NOTE-2004-01, ALEPH-2004-008, DELPHI-2004-042, L3-NOTE-2820, OPAL-TN-744, http://lephiggs.web.cern.ch/LEPHIGGS/papers/August2004_MSSM/index.html.
5. S. Chen *et al.* [CLEO Collaboration], Phys. Rev. Lett. **87** (2001) 251807 [arXiv:hep-ex/0108032]; P. Koppenburg *et al.* [Belle Collaboration], Phys. Rev. Lett. **93** (2004) 061803 [arXiv:hep-ex/0403004]. B. Aubert *et al.* [BaBar Collaboration], arXiv:hep-ex/0207076; E. Barberio *et al.* [Heavy Flavor Averaging Group (HFAG)], arXiv:hep-ex/0603003.
6. G. Bennett *et al.* [The Muon $g-2$ Collaboration], Phys. Rev. Lett. **92** (2004) 161802, hep-ex/0401008; G. Bennett *et al.* [The Muon $g-2$ Collaboration], Phys. Rev. D **73** (2006) 072003 [arXiv:hep-ex/0602035].
7. Z. Ahmed *et al.* [CDMS Collaboration], Phys. Rev. Lett. **102**, 011301 (2009).
8. J. Angle *et al.* [XENON Collaboration], Phys. Rev. Lett. **100**, 021303 (2008).
9. E. Aprile, L. Baudis and f. t. X. Collaboration, arXiv:0902.4253 [astro-ph.IM].
10. *SuperCDMS Development Project*, Fermilab Proposal 0947, October 2004.
11. J. R. Ellis, A. Ferstl, K. A. Olive and Y. Santoso, Phys. Rev. D **67** (2003) 123502 [arXiv:hep-ph/0302032].